ELSEVIER

Polymer 40 (1999) 4755–4761

polymer

Brillouin scattering and dielectric relaxation in PPG of different chain lengths and end groups

D. Engberg[a,*], J. Schüller[b], B. Strube[b], A.P. Sokolov[b], L.M. Torell[a]

[a]*Department of Experimental Physics, Chalmers University of Technology, S412 96 Gothenberg, Sweden*
[b]*Max Planck Institut für Polymerforschung, Mainz, Germany*

Received 15 September 1998; accepted 18 September 1998

Abstract

We have investigated the structural relaxational behavior of poly(propylene glycol), PPG, for polymer chains of increasing number of monomer units, $n(=3, 7, 70)$, and for different end groups (OH and CH_3) using Brillouin scattering and dielectric relaxation. In the case of the OH capped systems the relaxation dynamics are rather insensitive to chain length variations, whereas large effects are demonstrated when changing to CH_3 end groups. For chains with $n \lesssim 20$, there is a radical decrease in the sound velocity and the average relaxation time, when the hydroxyl terminations are replaced by methyl terminations. By using the nonpolar CH_3 endcapping the linking of adjacent chains, as is the case in the hydrogen bonded OH capped systems, is avoided.

Keywords: Brillouin scattering; Dielectric relaxation; Poly(propylene glycol)

1. Introduction

A polymer molecule can undergo many types of relaxation processes ranging from motions of only a few segments to those involving hundreds or more segments. As a result there is a wide distribution of relaxation times and the dynamics can be described by the connectivity constraints imposed on the monomers as they are connected to form the polymeric chain. In the simplest model, the characteristic times are given by the Rouse modes of the chain [1]

$$\tau_p \propto n_R^2/p^2 \quad (1)$$

where p is the index of a particular mode and n_R is the number of Rouse units in the chain, which is proportional to the number of monomer units, n, in the chain. Thus the longest relaxation time, $\tau_1 \propto n^2$, depends strongly on the chain length. The Rouse model usually gives an excellent description in the case of short chains. For chains that exceed a certain length, the so-called entanglement length, n_e, the dynamics are found to slow down dramatically. Then the interactions with surrounding chains set topological constraints to the motions of a polymer. The typical time for the onset of entanglement constraints is given by $\tau_e \sim n_e^2$. For relaxation to occur at times longer than τ_e the chain needs time enough to 'disentangle'. Then an overall diffusion of the whole chain is observed and it will mainly move along its own profile by reptation [2] with a characteristic time given by $\tau_d \propto n^3$.

The segmental relaxations that occur on a shorter time scale, $\tau < \tau_d$, than the reptational ones, are almost n independent for the entangled chains since they occur on a length scale shorter than the length of one chain. These, segmental processes, that are related to the glass transition dynamics, are the focus of the present study of poly(propylene glycol) (PPG).

In a previous light scattering study of PPG it was found that the structural relaxation time was independent of molecular weight in the range 425–10 000 ($n = 7170$) for hydroxyl terminated chains [3]. The surprising finding that light scattering results from such short chains are insensitive to the molecular weight, M_W, of the polymer has been suggested to be related to the terminating OH groups [3,4]. The polar end groups may be linked via hydrogen bonds between the chains. Thereby effectively longer chains are formed, which may explain the observed M_W independence.

The present work describes a Brillouin scattering and dielectric relaxation study of PPG, to understand the importance of chain length and termination, respectively, for the structural dynamics. In order to accomplish this we investigated PPG of chain lengths $n = 3$, 7 and 70 and we consider both hydroxyl and methyl terminated samples to examine the effect of hydrogen bonding.

* Corresponding author.

0032-3861/99/$ - see front matter
PII: S0032-3861(98)00704-6

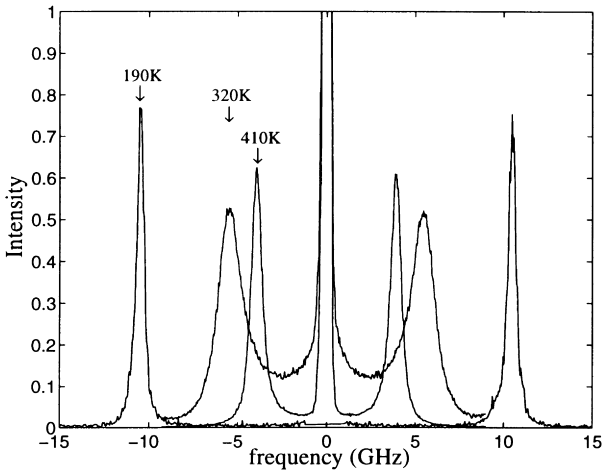

Fig. 1. Brillouin spectra below, close to, and above the temperature of maximum linewidth of OH terminated PPG of 70 monomer units.

2. Experimental techniques

2.1. Brillouin scattering

Brillouin scattering is the scattering of photons by acoustic phonons. A typical Brillouin spectrum [5] consists of Stokes and anti Stokes peaks, which are Doppler shifted to frequencies $\pm f_B$ from the elastic peak, see Fig. 1. The frequency shift is related to the sound velocity, v_s, via the equation

$$\omega_B = v_s q \tag{2}$$

where $\omega_B = 2\pi f_B$ is the angular frequency shift and $\boldsymbol{q} = \boldsymbol{k}_0 - \boldsymbol{k}_s$ is the momentum transfer to the sample. The change in magnitude of the wave vector of the incoming and scattered light, q is negligible and geometry arguments therefore allow us to write

$$q = |\boldsymbol{q}| = 2k_0 sin(\theta/2), \tag{3}$$

where θ is the scattering angle.

The width of the Brillouin peak is a measure of the damping of the acoustic phonons and strong damping leads to broader peaks. From the width of the spectral line the acoustic absorption coefficient, α, is given by

$$\alpha(\omega_B) = \Gamma_B / v_s(\omega_B), \tag{4}$$

where Γ_B is the halfwidth at halfheight in rad/s. In the present work we analyze the data in terms of the modulus. The zero frequency, or thermodynamic, modulus is related to the sound velocity via

$$M_0 = \rho v_s^2, \tag{5}$$

where ρ is the density of the sample. For a system subject to relaxation processes a complex frequency dependent modulus has to be used

$$M^*(i\omega) = M'(\omega) + iM''(\omega), \tag{6}$$

with the real and imaginary part denoted by [6]

$$M'(\omega) = \rho v_s^2(\omega) \tag{7}$$

$$M''(\omega) = \frac{2\rho}{\omega}\alpha(\omega)v_s^3(\omega). \tag{8}$$

The thermodynamic modulus [Eq. (5)] is then defined as the zero frequency limit of the real part. The imaginary part is a measure of the energy dissipation of the sound waves.

Generally the sound velocity, and thus the measured Brillouin frequency, is monotonically decreasing with increasing temperature and so is consequently the real part of the modulus. This decrease is simply indicating that the material becomes softer when the temperature is raised. In the temperature range where relaxing processes enter the Brillouin frequency window, the imaginary part of the modulus increases, goes through a maximum and then decreases again. The maximum occurs at the temperature when the inverse of the Brillouin frequency, $1/\omega_B$, is equal to the average structural relaxation time, $\langle\tau\rangle$. At this temperature, T_{max}, the probe frequency is at resonance with the system under study, i.e. the peak condition

$$\omega_B\langle\tau\rangle \approx 1 \tag{9}$$

is fulfilled and the energy dissipation is at its maximum. We deduce the average structural relaxation time at this temperature.

The relaxation function, $\phi(t)$, of the system can in the simplest case be expressed by an exponential function, i.e. using a single relaxation time τ according to

$$\phi(t) = \exp(t/\tau). \tag{10}$$

For most glass forming liquids the relaxation function is better described by a stretched exponential

$$\phi(t) = \exp[-(t/\tau_s)^\beta], 0 < \beta < 1, \tag{11}$$

and then the average relaxation time $\langle\tau\rangle$ is given by

$$\langle\tau\rangle = \frac{\tau_s}{\beta}\Gamma\left(\frac{1}{\beta}\right). \tag{12}$$

The parameter β describes the stretching, the smaller the value the more stretched is the function. The relaxation function is related to the reduced moduli, N' and N'' via a Fourier transform,

$$N'(\omega\tau) = \omega\tau\int_0^\infty \cos(\omega\tau x)\phi(x)dx \tag{13}$$

$$N''(\omega\tau) = \omega\tau\int_0^\infty \cos(\omega\tau x)\phi(x)dx \tag{14}$$

here x is a dimensionless integration variable. These analytical curves can be compared with experimental expressions for the reduced real and imaginary part of the

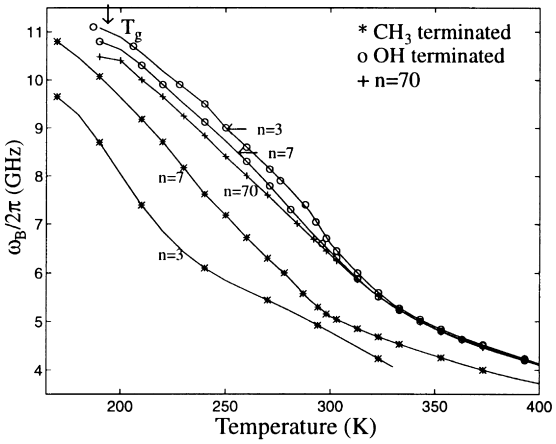

Fig. 2. Brillouin frequency shifts for OH and CH_3 capped PPG samples of different number of repeat units (n). The glass transition temperature for the OH capped systems is marked by a vertical arrow.

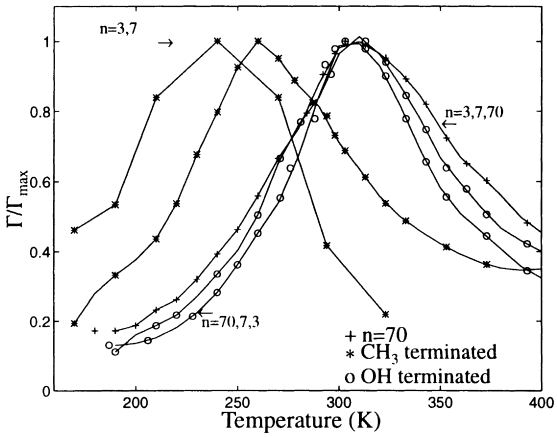

Fig. 3. Brillouin peak widths for OH and CH_3 capped PPG samples of different number of repeat units (n).

moduli. These are

$$N'(\omega) = \frac{M'(\omega) - M_0}{M_\infty - M_0} \tag{15}$$

$$N''(\omega) = \frac{M''(\omega)}{M_\infty - M_0} \tag{16}$$

where M_0 and M_∞ are the limiting zero and infinite frequency values of the moduli. The response at zero frequency is that of a fully relaxed system, see Eq. (5), and at infinite frequency there is no time for the system to relax so the response is that of a frozen system, fully elastic without any energy dissipation. We probe the relaxed system at high temperatures and the frozen system at low temperatures.

2.2. Dielectric relaxation

For a quantitative analysis of the complex permittivity $\epsilon = \epsilon' - \epsilon''$ the empiric Havriliak–Negami (HN) [7] function in conjunction with a conductivity term can be used

$$\varepsilon^*(\omega) - \varepsilon(\infty) = \frac{\Delta\varepsilon}{\left[1 + (i\omega\tau_{\mathrm{HN}})^{\alpha}\right]^{\gamma}} - \frac{i\sigma}{\varepsilon_0\omega^s} \tag{17}$$

The first term on the right-hand side describes the dielectric relaxation with a characteristic relaxation time, τ_{HN}, and with a relaxation strength $\Delta\epsilon$.The shape parameters α and γ ($0 < \alpha,\gamma \leq 1$) characterize the symmetrical and asymmetrical broadening of the loss peak, respectively. The case of a single exponential is restored if $\alpha = \gamma = 1$. The second term quantifies the DC conductivity σ, in terms of $\epsilon''(\omega)$, with a fit parameters $s < 1$. From fits according to Eq. (17), we determined τ_{HN}. Then, using the relationship between the stretched exponential and the Havriliak–Negami function given in Ref. [8] we calculate $\langle\tau\rangle$.

3. Experimental setup and samples

3.1. Sample preparation

The samples were PPG for which the monomer unit is $[OCH(CH_3)CH_2]_n$. Samples with $n = 3$, 7 and 70 were used. The OH terminated samples (from Polyscience Inc.) were degassed by repeated freeze–dry cycles on a vacuum line and then sealed in a cylindrical Pyrex™ cell for the light-scattering experiments. The samples used in the dielectric relaxation experiments were placed between the brass electrodes of a capacitor (diameter 30 mm, spacing ~ 100 μm), tightly surrounded by a Teflon™ cell. The CH_3 capped samples were prepared at the University of Oklahoma.

3.2. Brillouin scattering setup

The Brillouin scattering spectra were obtained at a scattering angle of 90° using a single. mode Argon ion laser delivering a power of 400 mW at 5140 Å. A six pass tandem Fabry–Pérot interferometer, model Sandercock [9], was used to frequency analyze the scattered light. A free spectral range of 20 GHz was used. Measuring in the GHz range at 90° means that we probe processes with characteristic times on the order of 10 ps and a momentum transfer of 0.002 $Å^{-1}$.

For the low temperature measurements the sample was kept in a liquid nitrogen cryostat. For the high temperature measurements an electrically heated furnace was used.

For the spectra obtained around $T_{\max}$, where the condition $\Gamma_B < \omega_B$ is poorly fulfilled an extra asymmetric term according to Ref. [6] was added in the analysis.

3.3. Dielectric relaxation

Dielectric measurements in the frequency range $10^{-2} - 10^6$ Hz were performed using a Solatron Schlumberger frequency response analyzer FRA 1260 equipped with a buffer amplifier of variable gain in order to determine the dielectric loss ϵ'' to within ± 3%. The sample temperature

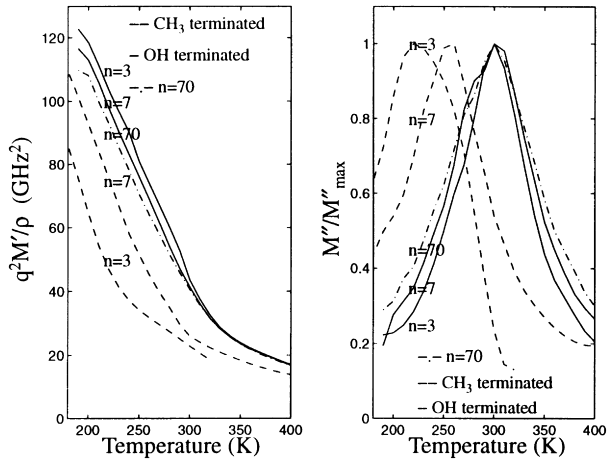

Fig. 4. The real (left) and imaginary (right) part of the modulus. Dashed lines are CH_3 capped samples, full lines are OH terminated samples and dotdashed the $n = 70$ sample.

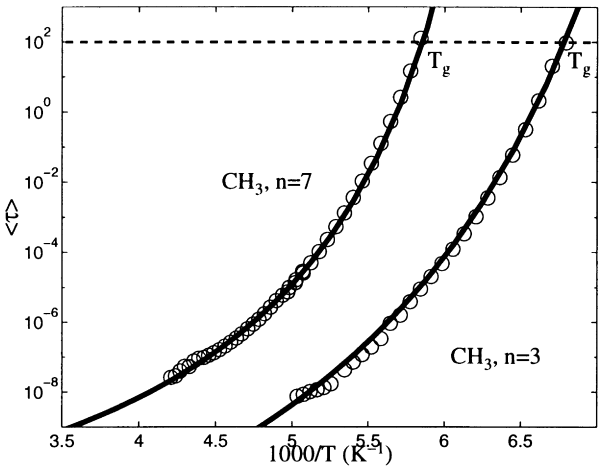

Fig. 6. Average dielectric relaxation times for CH_3 terminated PPG containing 3 and 7 monomer units. For the parameters of the VFT fit see Table 1. Dashed line at $\langle\tau\rangle = 100$ s represents the glass transition.

was controlled in the range 170–250 K by a nitrogen gas stream with a stability better than $\pm$ 0.1 K.

4. Results

4.1. Brillouin scattering

In Fig. 1 we present some typical Brillouin spectra chosen from the broad temperature range studied. It can be seen that the whole relaxation range is probed from the behavior of the Brillouin peak; being narrow at low temperatures and then increasing in width as the temperature is raised to become narrow again at higher temperatures. The phonon line width was deconvoluted with the instrumental function, and fitted with a Lorentzian. The measured Brillouin frequency shifts and widths for the OH and CH_3 terminated samples are shown in Figs. 2 and 3. It has been shown (C. Tengroth, L. Börjesson, D. Engberg, S. Howells, unpublished) that the termination has no influence on $n > 70$ samples. We therefore use the $n = 70$ sample as the high n limit for both OH and CH_3 terminated samples. In Fig. 2 the glass transition temperature T_g from the dielectric measurement is marked. We note that for the $n = 70$ sample we can identify a break in the temperature dependence at a temperature around T_g. Unfortunately we have too few data points to see this clearly for the other samples. The Brillouin data in Figs. 2 and 3 were used to calculate the modulus according to Eqs. (7) and (8), and the results are shown in Fig. 4. We actually plot the modulus times a factor q^2/ρ, but this factor does not change significantly over the measured range. In the case of the OH terminated samples we find that the data of the real part of the modulus, M', related to the Brillouin frequency, are indistinguishable at the higher temperatures of the relaxed system, i.e. independent of chain lengths, see Fig. 4. At lower temperatures we note that there is a small systematic variation in the data for the OH capped samples. The findings are however opposite the trend expected in the Rouse regime, the samples of smaller chain lengths demonstrate larger M' values. Turning to the imaginary part M'', which is related to the width of the Brillouin line, we notice that the temperature of maximum energy dissipation of the sound waves, T_{max}, changes very little as the molecular weight of the OH capped systems is changed. As the chain length decreases there is however a decrease in the width of M'' vs temperature, see the full lines on the right hand side of Fig. 4. For the CH_3 endcapped samples we find, contrary to the behavior of OH capped systems, a large decrease over the whole temperature range in the real part of the modulus, M', with decreasing chain length, see Fig. 4. This is to be expected in a non-entangled regime.

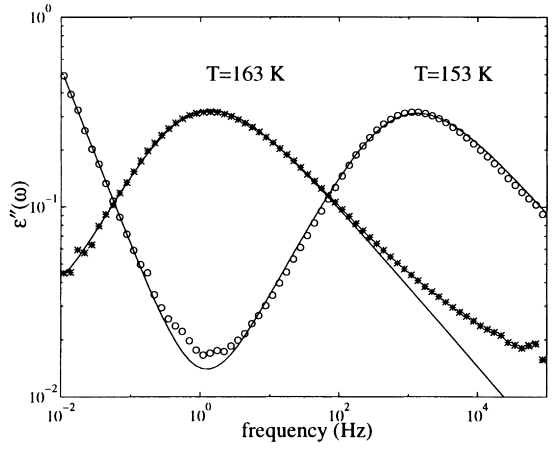

Fig. 5. Dielectric relaxation spectra of CH_3 terminated PPG with 3 monomer units obtained, at 153 and 163 K.

Further, for the imaginary part of the modulus we find that the position of T_{max} changes in an expected manner, i.e. the shorter chains have shorter relaxation times. The slight narrowing of the M'' vs T plot noted for the OH terminated samples was, however, not obvious in the CH_3 systems.

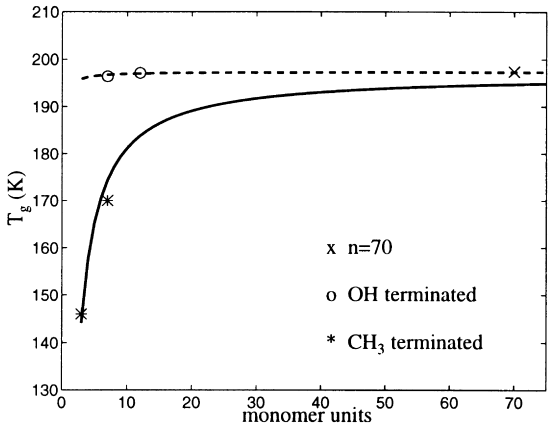

Fig. 7. Variation of T_g with chain length for hydroxyl [12] and methyl termination from dielectric measurements.

There is a weak tendency of narrowing but there are too few data points to conclusively reveal any change in shape of these curves.

4.2. Dielectric relaxation

In Fig. 5 we show typical dielectric relaxation spectra of the CH_3 terminated PPG with 3 monomer units. The dielectric loss for two temperatures and the corresponding Havriliak–Negami fits are shown. From Fig. 5 one notes that the peak position strongly depends on frequency and temperature, showing a shift in the maximum of the dielectric loss of three decades in frequency from a temperature change of only 10 K. In Fig. 6 we plot, for the CH_3 capped samples, the average relaxation time obtained from the peak frequency of the dielectric loss. Previous experiments on OH terminated PPG have shown a very weak dependence of the α-relaxation time on the chain length [10–12] and the glass transition temperature changes less than 1%. When the terminating OH group is replaced with a CH_3 group quite different results are obtained as seen in Fig. 6, the reduction of chainlength from $n = 7$ to $n = 3$ shifting the relaxation time by more than three decades.

The glass transition temperatures of the samples were deduced from the dielectric data as the temperature at which the relaxation time is 100 s. The resulting T_g values were found to be 147 and 170 K for CH_3 terminated PPG of chain length $n = 3$ and $n = 7$, respectively. The results can be compared with the glass transition temperature of 197 K as obtained independently of the chain length for the corresponding OH terminated PPG, see Fig. 7 which displays present and previously [12] obtained T_g data.

5. Discussion

5.1. Molecular weight and T_g

The local segmental dynamics, probed by light scattering, are the relaxation processes related to the glass transition. It is expected that for molecular weights below a crossover molecular weight, M_c, which is reported to be of the order 1000 [13] for lightscattering measurements, the glass transition temperature, T_g is molecular weight dependent and can be described by

$$T_g(M_W) = T_g(M_W = \infty) - \frac{c}{M_W} \tag{18}$$

where c is a material dependent constant.

In the OH terminated PPG there is however no change observed neither for T_g, see Fig. 7, nor for T_{max} see Fig. 4, as M_w decreases from 4000 ($n \approxeq 70$) to 200 ($n = 3$). The observation supports the previous findings on OH terminated PPG, see e.g. Refs. [3,10–12], that the segmental relaxation time is independent of molecular weight even though M_W decreases to values far below 1000. Transient crosslinks [4] cause the OH terminated systems to have an effective molecular weight much above that of a single chain, if studied on a timescale shorter than the transient crosslink. This results in the T_g behavior observed for the OH terminated PPG. We note a slight increase in the Brillouin observation of M' at low temperatures as M_W decreases, see Fig. 4, though T_g remains constant. We propose that the slight increase in M' comes from the fact that shorter chains have higher density of OH groups and that hydrogen bonds not only link but also locally stiffen the chain dynamics.

For the CH_3 endcapped PPG the dielectric data in Fig. 6 show that there is a decrease in T_g with decreasing molecular weight. The behavior is well described by Eq. (18) (see solid line in Fig. 7) with the T_g data of $n = 70$ as the high n limit. Such a molecular weight dependence of T_g is also revealed in the shift in temperature of M''_{max} as seen on the right-hand side of Fig. 4, which demonstrates a rapid change of T_{max} as the molecular weight is changed.

5.2. General form of τ vs T

We first discuss the relaxation time data of the OH terminated PPG of $n = 70$. In Fig. 8 we plot previous dielectric data [12] together with photon correlation spectroscopy results [14] and note good agreement between the data sets. Also included in Fig. 8 are Brillouin data as obtained in the present study from the spectrum at maximum energy dissipation (Eqs. (8) and (9)) and data from impulsive stimulated light scattering (ISS) [15] One notes the slight deviation when comparing the lightscattering (Brillouin) and dielectric results. This is to be expected for the high frequency (short time) regime since the two techniques respond to different relaxing entities, see e.g Ref. [16].

In Fig. 9 we compare data for the structural relaxational dynamics for the various systems of different chain length and end capping. We note in Fig. 9 that both the dielectric and light scattering data are independent of chain length for the OH terminated systems, while there are large changes of the relaxation times in the CH_3 systems. The data in Fig. 9

Table 1
VFT parameters. The experimental technique used is indicated as: Di dielectric, P photon correlation [14] and S impulsive stimulated lightscattering [15]

Technique	End	n	τ_0(fs)	D	T_0 (K)	T_g (K)
Di	CH_3	3	0.46	12.6	112	147
Di	CH_3	7	1051	6.8	141	170
Di	OH	7	—	8.3	160	197
Di	OH	70	171	7.0	165	197
P'S	OH	70	0.63	10.8	157	—

can be fitted to the Vogel Fulcher Tamman (VFT) [17] equation

$$\langle\tau\rangle = \tau_0 \exp\left(\frac{DT_0}{T - T_0}\right), \tag{19}$$

which generally is used to describe the relaxation dynamics of glass formers. Here T_0 is the high temperature fast relaxation time limit. D *is* a constant which can be taken as a measure of the fragility [18] of the system. The lower the D value the less resistant (more fragile) the system towards temperature induced changes and the larger is the departure from Arrhenius behavior. T_0 is a fitting parameter indicating the temperature where the relaxation time is expected to diverge.

The systems presently examined are all fairly fragile, having D values around 10. The fragility of the system only changes slightly as M_W changes, see inset Fig. 9, which shows the relaxation times in a T_g reduced representation, and Table 1.

5.3. The relaxation time distribution

The relaxation time distribution $\phi(t)$ is for glass formers

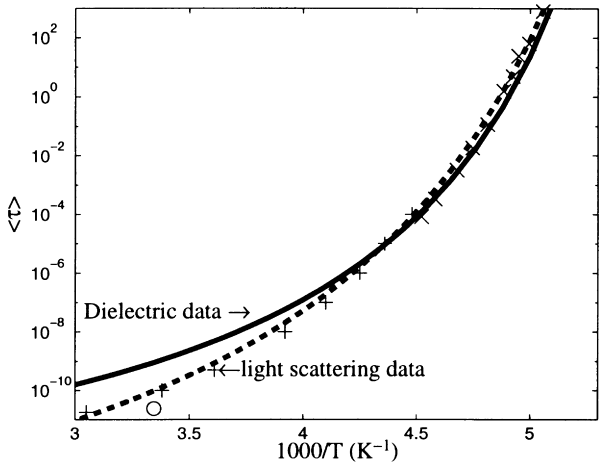

Fig. 8. Average relaxation time vs inverse temperature for PPG of $n = 70$. Full line represents aVFT fit of dielectric data [12]. Dashed line is from fits of photon correlation spectroscopy (×) [15] and impulsive stimulated light scattering (+) [15] and (○) represent present Brillouin scattering result. For the parameters of the fits see Table 1.

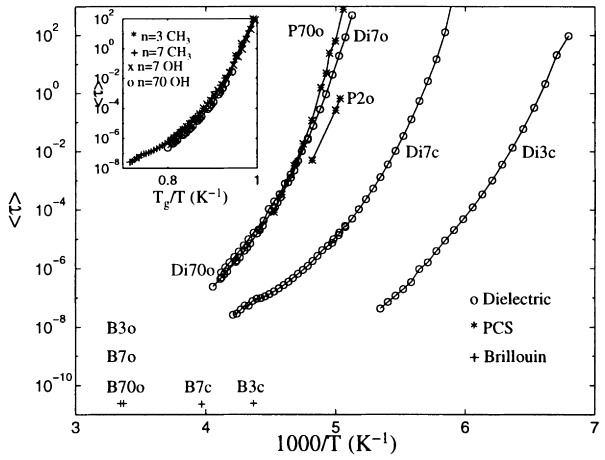

Fig. 9. Average relaxation time data vs inverse temperature. Circles correspond to dielectric data [12], (*) photon correlation spectroscopy data [13,19] and (+) Brillouin data. The different data sets are denoted with a capital letter for the technique used, Di for dielectric, P for photon correlation and B for Brillouin, followed by the number of monomer units and by o for OH terminated or c for CH_3 terminated chains. For VFT parameters see Table 1. Inset shows the corresponding T_g scaled results.

often expressed in terms of a stretched exponential

$$\phi(t) = \exp[(t/\tau)^{\beta}] \tag{20}$$

where τ is a characteristic relaxation time and $0 < \beta \leq 1$. The value of β is a measure of the width of the distribution, β being 1 for a single relaxation time. In Fig. 10 it can be seen that the Brillouin results for the reduced moduli of the OH terminated samples are all described by β parameters between 0.3 and 0.5. Photon correlation spectroscopy (PCS) measurements give for OH terminated PPG of $n = 70$ a distribution parameter of $\beta \approx 0.4$ independent of temperature [14]. For the OH terminated dimer PCS data show that β increases [20], i.e. the distribution of relaxation times narrows when the chains becomes shorter. In Fig. 4 we also note that the width of the peak in the imaginary part

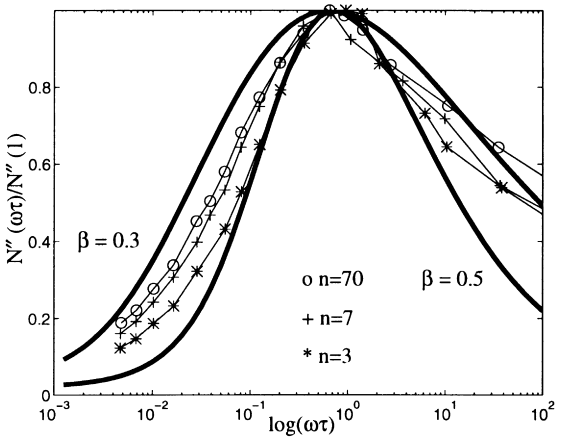

Fig. 10. Reduced modulus data from Brillouin scattering for OH terminated PPG of monom units $n = 3$, 7, 70. The full lines are calculated values for $\beta = 0.3$ and 0.5.

of the modulus vs temperature becomes narrower when the number of monomer units decreases. This observation can be explained by two different effects; a faster variation of the relaxation time with temperature or a more narrow distribution of relaxation times for the shorter systems. The latter is in accordance with our analysis. Dielectric relaxation shows only small changes in fragility, i.e. the temperature behavior of the relaxation time, see inset of Fig. 8, which suggests that it is the distribution of relaxation times which narrows as the molecular weight decreases. This is in accord with the PCS results [20] and also with dielectric relaxation measurements [19]. The physical background may again be the stiffening of the chains via the OH bonding which becomes more effective for shorter chains. It is also demonstrated by the increase in the Brillouin frequency, see Fig. 2. As the system stiffens it loses some of its relaxational channels and as a result we observe a narrowing of the relaxation time distribution.

We expect that the distribution of relaxation times narrows with decreasing M_W also for the CH_3 capped samples but we lack enough data to make any quantitative analysis.

6. Conclusions

We have studied the relaxation dynamics of CH_3 and OH terminated PPG chains of various chain lengths by dielectric relaxation and Brillouin scattering. We find that the CH_3 terminated chains behave with a chain length dependence according to that of polymers in general; the T_g values and the average relaxation times decrease as the molecular weight decreases.

For the OH terminated PPG, hydrogen bonds cause a quite different behavior. OH end links between the end groups of the chains result in an effective chain length much above that of the individual chains. When the effective chain length is above the length needed for the onset of entanglement dominated dynamics we do not, however, probe the very slow reptational dynamics but the faster segmental motions of sections of the polymer chain. Only probing part of the chain means that the relaxation time we measure is almost independent of chain length. We also note from the sound velocity that this linking by OH groups stiffens the chain. This effect is stronger at lower temperatures which can be explained by the fact that the links and bondings are then the least disturbed.

A stiffer chain has lost some of its relaxational channels and we therefore expect the distribution of relaxation times to become more narrow, an effect demonstrated in the narrowing of the imaginary part of the modulus.

Acknowledgements

The hospitality of the MaxPlanck Institut für Polymerforschung in Mainz is acknowledged by D.Engberg. Sample preparations by professor R.Frech, University of Oklahoma is also gratefully acknowledged. This work was supported by the Swedish Science Research Council.

References

[1] Rouse P. J Chem Phys 1953;21:1273.
[2] de Gennes P. J Chem Phys 1971;55:572.
[3] Borjesson L, Stevens J, Torell LM. Polymer 1987;28:1803.
[4] Heinrich G, Alig I, Donth E. Polymer 1988;29:1198.
[5] Pinnow D, Candau S, LaMacchia J, Litovitz T. J Acoust Soc Am 1968;43:131.
[6] Montrose G J, Solovyev V A, Litovitz T A. J Acoust Soc Am 1968;43:117.
[7] Havriliak S, Negami S. Polymer 1967:101.
[8] Alvarez F, Alegrifa A, Colmenero J. Phys Rev 1991;B44:7306.
[9] Sandercock JR. In: Murphy WF, editor. The 7th international conference on Raman spectroscopy. Amsterdam: NorthHolland, 1980:364.
[10] Schlosser E, Schönhals A. Progr Colloid Polym Sci 1993;91:158.
[11] Baur M, Stockmayer W. J Chem Phys 1965;43:4319.
[12] Schüller J, Mel'nichenko Y, Richert R, Fischer E. Phys Rev Lett 1994;73:2224.
[13] Jacobson P, Börjesson L, Torell L M. J Non-Cryst Solid 1991;131–133:104.
[14] Sidebottom D, Bergman R, Börjesson L, Torell M. Phys Rev Lett 1992;68:3587.
[15] Duggal A, Nelson K. J Chem Phys 1991;94:7677.
[16] Berne BJ, Pecora R. Dynamic light scattering. New York: Wiley, 1976.
[17] Vogel H. Phys Z 1921;22:645.
[18] Angell CA. In: Ngai KL, Wright GB, editors. Relaxation in complex systems. Washington, DC: Office of Naval Research, 1984:3.
[19] Mel'nichenko YB, Schuller J, Richter R, Ewen B, Loong C-K. J Chem Phys 1995;103:2016.
[20] Bergman R, Svanberg C, Anderson D, Brodin A, Tovell LM. J Non-Cryst Solid 1998;235–237:225.